Identification of a novel motif that affects the conformation and activity of the MARCH1 E3 ubiquitin ligase

Marie-Claude Bourgeois-Daigneault and Jacques Thibodeau*

Département de Microbiologie et Immunologie, Université de Montréal, Montréal, QC, Canada

*Author for correspondence (jacques.thibodeau@umontreal.ca)

Accepted 21 November 2012
Journal of Cell Science 126, 989–998

doi: 10.1242/jcs.117804

Summary

MARCH1, a member of the membrane-associated RING-CH family of E3 ubiquitin ligases, regulates antigen presentation by downregulating the cell surface expression of Major Histocompatibility Complex class II and CD86 molecules. MARCH1 is a transmembrane protein that exposes both its N- and C-terminus to the cytoplasm. We have conducted a structure–function analysis of its two cytoplasmic tails to gain insights into the trafficking of MARCH1 in the endocytic pathway. Fusion of the N-terminal portion of MARCH1 to a type II transmembrane reporter molecule revealed that this cytoplasmic tail contains endosomal sorting motifs. The C-terminal domain also appears to contain intracellular sorting signals because it reduced surface expression of a type I transmembrane reporter molecule. Mutation of the two putative C-terminal tyrosine-based sorting signals did not affect the activity of human MARCH1; however, it did reduce its incorporation into exosomes. Moreover, site-directed mutagenesis pointed to a functional C-terminal $_{221}$VQNC$_{224}$ sequence that affects the spatial organization of the two cytoplasmic regions. This motif is also found in other RING-type E3 ubiquitin ligases, such as parkin. Altogether, these findings highlight the complex regulation of MARCH1 trafficking in the endocytic pathway as well as the intricate interactions between its cytoplasmic tails.

Key words: E3 ubiquitin ligase, MARCH1, Major Histocompatibility Complex (MHC)

Introduction

The intracellular trafficking of Major Histocompatibility Complex class II molecules (MHC II) has been extensively studied in various species and types of APCs. Synthesized in the ER, MHC II heterodimers assemble with the invariant chain (Ii) and cross the Golgi apparatus before ultimately reaching the endosomes (Landsverk et al., 2009; Berger and Roche, 2009). It is believed that a fraction of the newly synthesized MHC II/Ii pool associates with the clathrin adaptor AP-1 and reaches early endosomes directly from the trans-Golgi network (Salamero et al., 1996; Brachet et al., 1999). However, most complexes appear to first reach the plasma membrane through the default secretory pathway. At the cell surface, the leucine-based cytoplasmic motifs of Ii are recognized by AP-2 and the cargo is internalized through clathrin-coated vesicles (Dugast et al., 2005; McCormick et al., 2005). Once in the endocytic pathway, the MHC II/Ii complex ultimately reaches acidic compartments where Ii is degraded (Cresswell, 1996). A variety of non-cysteine proteases, including AEP, are capable of cleaving the luminal part of Ii to generate a 22 kDa fragment (p22) (Manoury et al., 2003). Then, cysteine proteases sequentially generate p10 and the class II-associated invariant chain peptide (CLIP), which remains associated with MHC II (Hsing and Rudensky, 2005). The exchange of CLIP for an antigenic peptide is mediated by the non-classical MHC II molecule human leukocyte antigen (HLA)-DM and terminates the association of Ii and MHC II (Denzin and Cresswell, 1995). The peptide–MHC II complex is then free to go to the cell surface (Landsverk et al., 2009). After being displayed at the plasma membrane, peptide-loaded MHC II molecules are endocytosed in sorting endosomes through an ARF6-dependent clathrin-independent mechanism and most complexes are returned to the cell surface via recycling tubular endosomes (Walseng et al., 2008).

Recently, it has been shown that ubiquitylation participates in the intracellular trafficking of MHC II, especially in resting cells or under immunosuppressive conditions (Shin et al., 2006; van Niel et al., 2006; De Gassart et al., 2008; Thibodeau et al., 2008; Matsuki et al., 2007). Ubiquitylation is a well-known post-translational protein modification that leads to many different effects, from endocytosis and vesicular trafficking to degradation and regulation of the cell cycle (Adhikari and Chen, 2009). The attachment of ubiquitin on a substrate involves three players: First, the activating enzyme (E1) activates free ubiquitins. Second, the activated moiety interacts with an ubiquitin-conjugating enzyme (E2) (Ye and Rape, 2009). Then, the E2s associate with ubiquitin ligases (E3), which recognize and modify the appropriate targets (Deshaies and Joazeiro, 2009).

The membrane-associated RING-CH (MARCH) protein family includes nearly a dozen E3 ubiquitin ligases that target important players of the immune response (Ishido et al., 2009). Most of the RING-type E3 ubiquitin ligases are cytoplasmic or nuclear proteins (Lehner et al., 2005). With the exception of MARCH7 and MARCH10, MARCH family members are

Journal of Cell Science

multi-pass transmembrane proteins (Wang et al., 2008; Nathan and Lehner, 2009). MARCH1 shares many targets with MARCH8, its closest family member. MHC II, CD86, transferrin receptor, HLA-DM and Fas were all reported to be ubiquitylated and downregulated from cell surface by MARCH1 and MARCH8 (Bartee et al., 2004; Ohmura-Hoshino et al., 2006; Matsuki et al., 2007; Jahnke et al., 2012). While MARCH1 expression is restricted to secondary lymphoid organs (Bartee et al., 2004), it can be induced or repressed by different stimuli. For example, we have shown that IL-10 modulates its expression in human primary monocytes and mouse B cells (Thibodeau et al., 2008; Galbas et al., 2012). In addition, many groups have demonstrated that LPS-induced maturation of dendritic cells repressed MARCH1 expression, allowing the cell surface expression of newly synthesized MHC II molecules (Ohmura-Hoshino et al., 2006; De Gassart et al., 2008; Walseng et al., 2010; Tze et al., 2011; ten Broeke et al., 2011).

While the overall structure of MARCH1 and the function of its RING domain are well defined, the other parts of the molecule remain to be fully characterized. The RING domain, localized in the cytoplasmic N-terminal region participates in the ubiquitin transfer from the E2 to its substrate (Deshaies and Joazeiro, 2009). A study about the viral homologue mK3 has highlighted the importance of the DIRT domain, i.e. the domain localized between the RING and the first transmembrane, which is involved in substrate recognition (Cadwell and Coscoy, 2008). Also, the group of Lybarger reported the presence of C-terminal cytoplasmic endosomal sorting motifs in murine MARCH1 (mMARCH1) (Jabbour et al., 2009). Other key regions in MARCH proteins include their transmembrane domains, which are implicated in target recognition and dimer formation (Lehner et al., 2005; Corcoran et al., 2011; Bourgeois-Daigneault and Thibodeau, 2012). We have recently demonstrated that dimerization allows autoregulation of MARCH1 through ubiquitylation (Bourgeois-Daigneault and Thibodeau, 2012).

The fine details of the spatiotemporal interaction between MARCH1/8 and MHC II remain to be characterized. Early studies suggested that MARCH8 ubiquitylates its targets at the plasma membrane and induces their rapid endocytosis (Ohmura-Hoshino et al., 2006). In mouse primary B cells, it appears that ubiquitylated MHC II molecules can be immunoprecipitated from the plasma membrane. Also, in MARCH1-deficient B cells, the cell-surface MHC II molecules were shown to be stabilized (Matsuki et al., 2007). These results contrast with those obtained in DCs where no difference in the kinetics or mode of MHC II internalization was observed between MARCH1-deficient and -proficient mouse cells (Matsuki et al., 2007; Jabbour et al., 2009). A recent study by Eyster et al. also demonstrated that ubiquitylation of different targets by MARCH1 and 8 would affect their trafficking at the level of recycling endocytic structures, preventing their return to the plasma membrane (Eyster et al., 2011).

The expression of MARCH1 is closely regulated and very low levels of the protein are detectable in primary cells (Matsuki et al., 2007). MARCH1 can ubiquitylate a variety of unrelated cytoplasmic domains and part of the specificity most likely arise from the tight compartmentalization of the enzyme. To clarify the mechanisms by which MARCH1 mediates the intracellular retention of MHC II, we further characterized the structure–function properties of the two MARCH1 cytoplasmic domains using reporter molecules and site-directed mutagenesis. Our results highlighted the presence of a short functional C-terminal amino acid sequence (VQNC) that is conserved in other E3 ubiquitin ligases and which appears to interact with the N-terminal cytoplasmic tail, close to the RING domain.

Results

MARCH1 is not active in the biosynthetic pathway

Some members of the MARCH-like family of ubiquitin ligases, such as mK3 and MARCH6, modify their targets in the ER (Boname et al., 2004; Kreft et al., 2006). Indeed, mK3 inhibits antigen presentation by ubiquitylating MHC class I molecules and causing their degradation through the ERAD (ER-associated degradation) pathway (Boname et al., 2004). Also, MARCH2, 3, 4 and 9 appear to be located along the biosynthetic and secretory pathways, including the trans-Golgi network (Bartee et al., 2004). We have addressed the possibility that ubiquitylation of MHC II in the ER might play a role in the downregulation of surface expression. We generated an ER-retained MARCH1 mutant by deleting the last 40 amino acids of the C-terminal cytoplasmic tail (Fig. 1A,B). This MARCH1Δ40 variant (called $M1_{KKxx}$) ends with the sequence KKLE, creating a classical di-lysine (KKxx) ER-retention motif (Nilsson et al., 1989). Indeed, immunofluorescence microscopy showed that the $M1_{KKxx}$ mutant colocalized with calnexin and was confined to the ER in transfected HeLa cells (Fig. 1C, upper panels). The MARCH1 constructs used in this study are tagged at their N-terminus with YFP to facilitate their detection. The expression of the untagged MARCH1 is weak and the fusion with the YFP stabilizes the molecule without affecting the function (Bourgeois-Daigneault and Thibodeau, 2012). To test the impact of mislocalization, $M1_{KKxx}$ was transiently transfected in CIITA-expressing cells and the surface expression of MHC II was monitored by flow cytometry. A control MARCH1 lacking two additional residues (M1Δ42) was generated in order to inactivate the ER retention motif (Fig. 1A,B). Indeed, confocal microscopy experiments show M1Δ42 in $CD63^+$ endosomal vesicles (Fig. 1C, bottom panels). Fig. 1D shows that, as compared to wild-type MARCH1 (YFP–MARCH1) or M1Δ42, which both efficiently downregulate MHC II from the cell surface, the ER-retained $M1_{KKxx}$ was totally inactive. As it has been suggested previously that MARCH1 does not target MHC II/Ii complexes (Shin et al., 2006), the possibility remained that Ii created steric hindrance, thereby preventing ubiquitylation of MHC II cytoplasmic domains in the ER. Thus, we compared the activity of the deleted MARCH1 molecule in cells stably expressing only HLA-DR1. Fig. 1E shows that, as compared to cells expressing the control YFP (left panel), only the WT MARCH1 was able to downregulate cell surface MHC II expression. Altogether, these results show that MARCH1 does not act from the ER.

MARCH1 and MHC II interact in the endocytic pathway

Recent results have shown that MARCH1 does not affect the kinetics of MHC II endocytosis from the plasma membrane (Walseng et al., 2010). Coupled to the fact that clathrin-independent endocytosis of specific cargo proteins is not affected by the expression of MARCH1, these results suggest that ubiquitylation occurs in endocytic vesicles (Eyster et al., 2011). To gather further evidence for an interaction between MHC II and MARCH1 in vesicles, we have used photobleaching FRET digital imaging microscopy in live HeLa cells to detect proximity between transiently transfected GFP_2-MARCH1 and DRα/β-YFP (Fig. 2A). As a negative control, we used HeLa cells

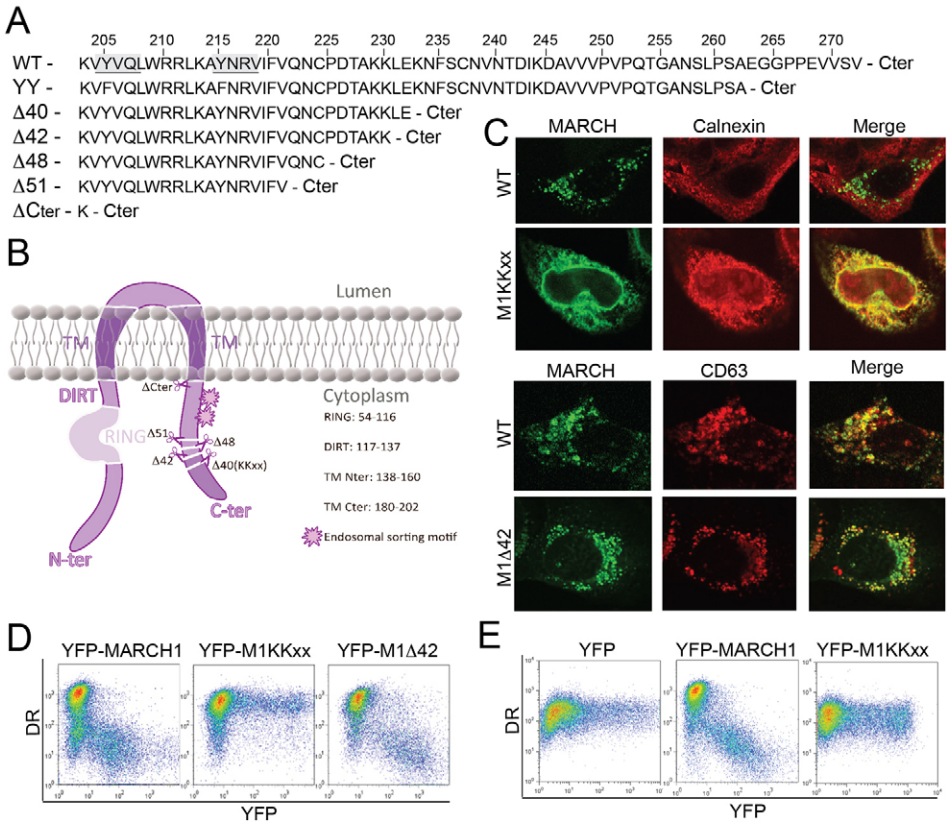

Fig. 1. MARCH1 does not prevent the cell surface expression of MHC II in the endoplasmic reticulum. (**A**) Sequence alignment of the C-terminal cytoplasmic portions of the MARCH1 mutants used in this study. The underlined shaded sequences are the predicted tyrosine-based sorting motifs. (**B**) Schematic representation of the MARCH1 mutants used in this study. (**C**) Confocal microscopy analysis of HeLa cells transfected with YFP-M1KKxx, YFP-MARCH1 or YFP-M1Δ42 and stained for calnexin or CD63. (**D**) HEK 293E CIITA cells were transfected with YFP-MARCH1, YFP-M1KKxx or YFP-M1Δ42 and analyzed by flow cytometry for the surface expression of DR. (**E**) HeLa DR1 cells were transfected with YFP, YFP-MARCH1 or YFP-M1KKxx and stained for the cell surface expression of DR. Data are representative of at least two experiments.

transfected with DRα, DRβ-YFP and DRβ-GFP_2 (Fig. 2B), the rationale being that these two β chains will be found in the same compartments but will not interact in the absence of invariant chain. Fig. 2 shows two series of images of the same cells for each condition, one preceding (pre-bleach) and the other following (post-bleach) bleaching of the selected areas. Prior to bleaching, a weak signal is observed for GFP_2–MARCH1, which colocalizes with the strong signal observed for DRβ–YFP (Fig. 2A, upper panels). The FRET signal represents the detection of the fluorescence emitted by the YFP after laser excitation of the GFP_2. This signal reflects the transfer of energy that occurs when the two molecules are close one to the other. However, as the intensity of the FRET signal is highly dependent on the relative concentration of the tagged molecules even in conditions where the two do not interact, the intimate contact is more accurately assessed through the loss of donor fluorescence upon quenching by the associated acceptor molecule (Szöllosi et al., 1998). Indeed, instead of being released as a detectable fluorescence signal, the energy emitted by the GFP_2 upon stimulation will be absorbed and quenched by the YFP in conditions where the two molecules are in contact, thereby explaining the weak signal detected for GFP_2 in the vesicles where DRβ accumulated in large amount. To release this fluorescence (de-quenching), selected areas showing strong YFP and FRET signals were bleached (white dashed box). In these conditions, the YFP cannot accept or emit energy. Fig. 2A shows that subsequent to the bleach, an important augmentation of the fluorescence emitted by GFP_2 correlated to a complete disappearance of the YFP signal in the bleached areas (Fig. 2A, bottom panels). The release of the GFP_2 fluorescence confirms the close proximity of the two molecules. On the other hand, the cells expressing DRα, DRβ–YFP and DRβ–GFP_2 showed a different pattern (Fig. 2B). Prior to bleaching, a strong signal was detected for both GFP_2, YFP and the FRET in the same vesicles (upper panels). In line with an absence of specific interaction, the molecules are located in the same compartments, but the signal of the GFP_2 is not quenched by the close proximity of the YFP. Indeed, bleaching of a selected region did not result in an augmentation of the GFP_2 signal (bottom panels), but instead resulted in a complete disappearance of the signals. These results showing a specific MARCH1–MHC II interaction in vesicles are in line with a model where internalized cargo proteins are ubiquitylated in sorting vesicles and redirected deeper into the endocytic pathway (Eyster et al., 2011).

Endosomal sorting elements in the C-terminal cytoplasmic domains

A recent study reported the presence of two tyrosine-based endosomal sorting motifs in the C-terminal cytoplasmic domain of mouse MARCH1 and human MARCH8 (Ohmura-Hoshino et al., 2006; Goto et al., 2008; Jabbour et al., 2009). In line with the presence of sorting motifs within the molecule, we and others have shown that human MARCH1 is localized into CD63 and LAMP-1 positive endosomal vesicles (Bartee et al., 2004; Bourgeois-Daigneault and Thibodeau, 2012). To further characterize the functional motifs in the C-terminal cytoplasmic portion of human MARCH1, we used DR as a reporter molecule and replaced the DRβ cytoplasmic tail with the C-terminal domain of MARCH1. This DRβ-M1 chimeric chain was transiently transfected in HEK 293T along with DRα (DR-M1) and the expression of DR was analyzed by flow cytometry. Fig. 3A reveals that, as compared to wild-type DR, the DR-M1 heterodimer is not as efficiently

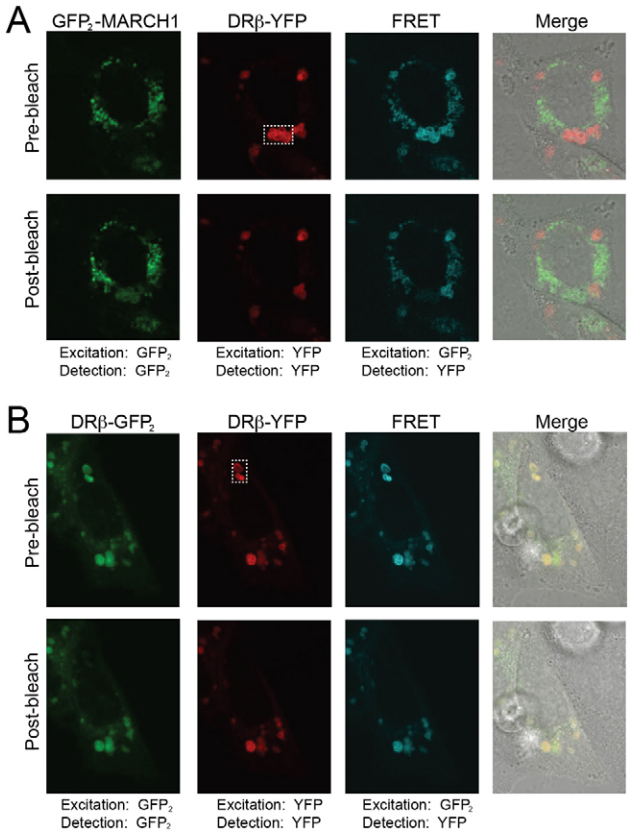

Fig. 2. MARCH1 and HLA-DR interact in intracellular vesicles. HeLa cells on coverslips were transfected with (**A**) GFP_2-MARCH1, DRα and DRβ-YFP or (**B**) DRβ-GFP_2, DRα and DRβ-YFP. After 48 hours, confocal microscopy images of live cells were taken. A first series of images (upper panels) were taken before bleaching of defined areas (white dashed boxes). Then, a second series of images were taken (bottom panels). The experiment is representative of three independent experiments.

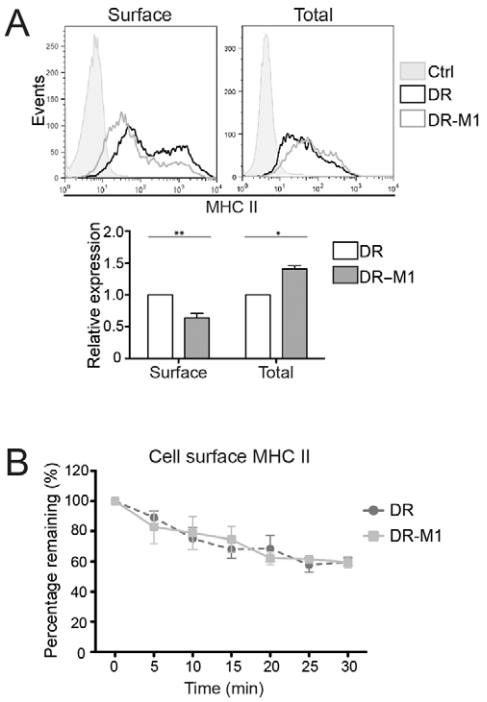

Fig. 3. The C-terminal cytoplasmic domain of MARCH1 encodes functional sorting elements. (**A**) HEK 293T cells transfected or not (Ctrl) with DRα and with either DRβ or DRβ-M1. After 48 h, cells were analyzed by flow cytometry for DR expression before (surface) or after (total) membrane permeabilization. The averages of the MFVs obtained for four different experiments were plotted as a bar chart. Values are relative to the fluorescence of wild-type DR (bottom panel). (**B**) HEK 293T cells were transfected with DRα and either DRβ or DRβ-M1. After 24 h, cells on ice were stained with an MHC II-specific antibody. The cells were then washed and incubated at 37°C for various times from 0 to 30 minutes prior to staining with the secondary antibody and flow cytometry analysis. The data combines the values obtained from four different transfections. Student's *t*-test was performed; $*P \leq 0.001$ and $**P \leq 0.005$.

expressed at the cell surface (upper left and bottom panels). This is not due to lower transfection efficiency as the total amount of molecules detected after permeabilization is greater for DR-M1 (upper right and bottom panels). Of note, the mean fluorescence values (MFV) measured after membrane permeabilization (total DR) are generally reduced as compared to those obtained for cell surface molecules. This is due to the high fluorescence background arising from cell fixation and permeabilization.

We hypothesized that enhanced internalization could explain the weaker cell surface display of DR-M1. To test this possibility, we conducted a flow-cytometry-based endocytosis assay. MHC II-transfected HEK 293T cells were incubated with L243 and the internalization of the monoclonal antibody at 37°C was monitored over time. Fig. 3B shows that the chimeric DR-M1 and wild-type DR were internalized at the same pace, suggesting that any sorting signal enclosed in the DR-M1 chimeric molecule does not affect endocytosis.

Differential role of the tyrosine-based motifs in mouse and human MARCH1

The previous experiments are in line with the presence of sorting elements within the C-terminal cytoplasmic domain of human MARCH1. Knowing the importance of the tyrosine-based endosomal sorting signals for the function of human MARCH8 and mouse MARCH1, we investigated the functionality of these conserved motifs in human MARCH1. The two key tyrosine residues were changed for phenylalanines by site-directed mutagenesis (M1Y205F and M1Y215F). A mutant with both tyrosines mutated (M1YY) was also generated. Also, the corresponding mutations were introduced in human MARCH8 and mouse MARCH1. The activity of these YFP-tagged MARCH variants was tested in HEK 293E CIITA cells for the downregulation of surface MHC II. Our results confirmed the importance of tyrosine 222 for mouse MARCH1 (data not shown) and human MARCH8 (Fig. 4A). As negative control, a MARCH8 variant devoid of its catalytic RING domain (M8ΔRING) was used. Our results clearly show that the tyrosine 222 is important for the activity of MARCH8. Importantly, these results demonstrate that overexpression of the transfected molecules does not preclude the study of trafficking motifs. Goto et al. had shown previously that deletion of either tyrosine motif affected the function of MARCH8 (Goto et al., 2008). However, our results demonstrate that only the N-terminal motif is critical. This discrepancy is probably due to the nature of the alterations as deletion by Goto et al. deleted the four residues constituting the

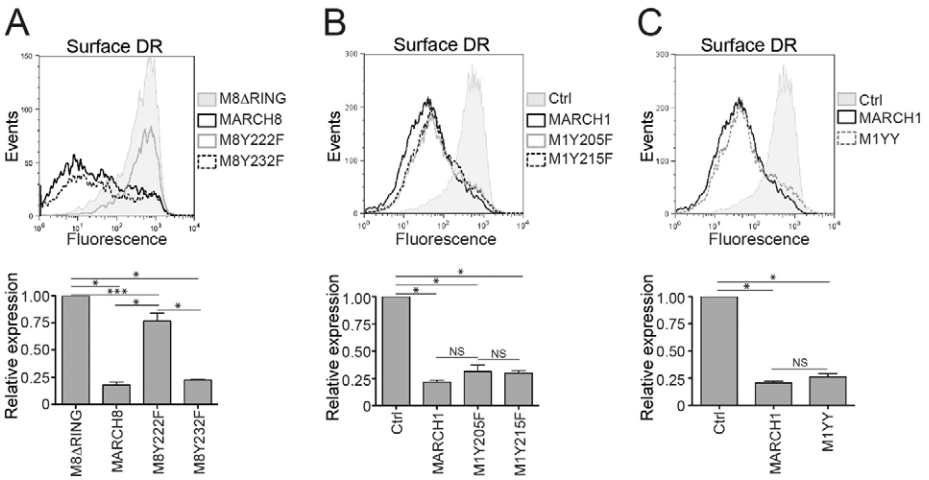

Fig. 4. The tyrosine sorting motifs of human MARCH1 are dispensable for the downregulation of MHC II. (**A–C**) Flow cytometry analysis showing MHC II expression at the surface of YFP-positive HEK 293E CIITA cells transfected with YFP-M8ΔRING, YFP-MARCH8, YFP-M8Y222F or YFP-M8Y232F (A), YFP, YFP-MARCH1, YFP-M1Y205F or YFP-M1Y215F (B), or YFP, YFP-MARCH1 or YFP-M1YY (C). The MFVs obtained from four different experiments were averaged and divided by those of YFP-M8ΔRING (A) or YFP (B,C) and represented as bar charts (bottom panels). Student's *t*-test was performed; $*P \leq 0.001$, $**P \leq 0.005$, $***P \leq 0.1$; NS, no significant difference.

putative C-terminal (Goto et al., 2008). For MARCH1, neither the Y205 nor Y215 residue appeared important for the downregulation of MHC II expression (Fig. 4B,C). Thus, our results highlight some structure-function differences between highly conserved MARCH family members.

The tyrosine-based endosomal sorting motifs of MARCH1 affect its trafficking

Our above-described analysis suggested that the tyrosine motifs are not required for the downregulation of MHC II. Also, mutation of the tyrosine motifs did not affect the co-localization with CD63, a marker for late endocytic compartments (Fig. 5A).

As tyrosine-based sorting signals affect the incorporation of many endosomal proteins into exosomes (Théry et al., 2002), we investigated the presence of YFP, YFP–MARCH1 and the YFP–M1YY proteins into the microvesicles shed from transfected cells. HEK-293T-cell-derived exosomes were purified from the culture media by ultracentrifugation. The cells and the exosomes, the latter coupled to latex beads, were analyzed by flow cytometry for YFP expression. Our results showed a complete absence of YFP in exosomes even though the protein is expressed at high levels upon transient transfection (Fig. 5B, upper panel). In contrast, YFP–MARCH1 and YFP–M1YY were both found in exosomes. To compare the sorting efficiency of the various molecules, we calculated a fluorescence ratio between cells and exosomes. The analysis corroborated the absence of YFP from exosomes, but revealed a significant reduction in the incorporation of YFP–M1YY as compared to YFP–MARCH1 (Fig. 5B, bottom panel). These data suggest that the tyrosine motifs are functional and finely tune the trafficking of MARCH1.

To investigate whether the tyrosine-based motifs in the C-terminal cytoplasmic portion of DR-M1 are responsible for the intracellular accumulation described above (Fig. 3A), we mutated the two tyrosines (DRβ-M1YY) and tested the impact on surface expression in transfected cells. The surface and total expression of DR-M1YY was compared to DR-M1 and DR by

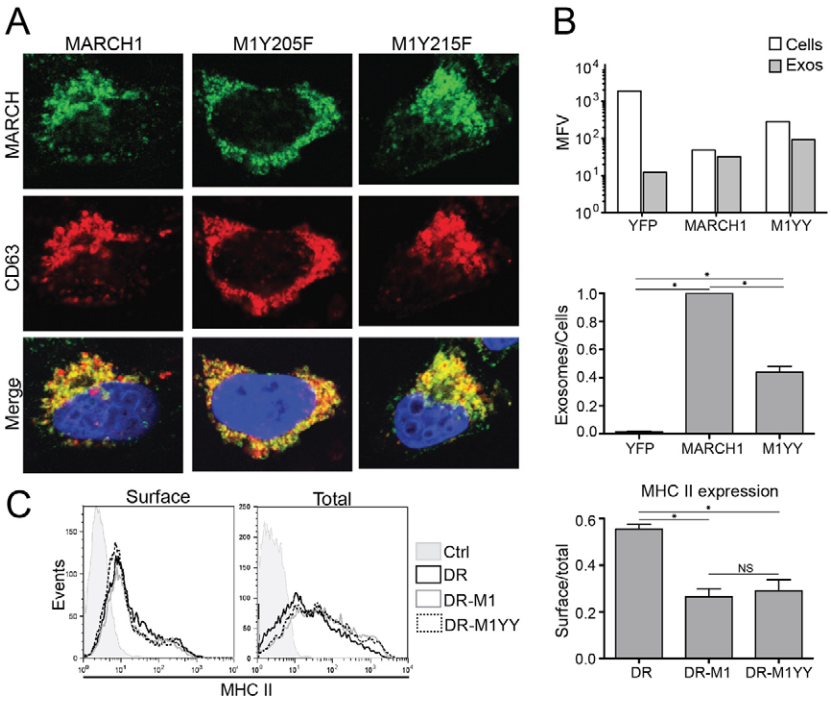

Fig. 5. The tyrosine sorting motifs of human MARCH1 are functional. (**A**) Confocal microscopy analysis of HeLa cells transfected with YFP-MARCH1, YFP-MARCH1Y205F or YFP-M1Y215F and stained for CD63. (**B**) HEK 293T cells were transfected with YFP, YFP-MARCH1 or YFP-M1YY and after 48 hours, the cells were analyzed by flow cytometry. The secreted exosomes were collected, coupled to beads and analyzed by flow cytometry. The upper panel shows the MFVs obtained for cells and the exosomes in each condition for one representative experiment. The bottom panel shows a ratio of the YFP MFVs divided by those obtained for MARCH1, averaged from two different experiments. (**C**) HEK 293T cells were transfected or not (Ctrl) with DRα and with either DRβ, DRβ-M1 or DRβ-M1YY. After 48 hours, cells were analyzed by flow cytometry for DR expression before (surface) or after (total) membrane permeabilization. The right panel shows a ratio of the surface MFVs divided by the averaged total MFVs from four different experiments. Student's *t*-test was performed; $*P \leq 0.001$; NS, no significant difference.

flow cytometry (Fig. 5C). Because the three constructs are not expressed at the exactly same levels, we expressed the results as the proportion of total molecules that are found at the plasma membrane (surface/total). These ratios clearly show that the intracellular accumulation of DR-M1 is not caused by the tyrosine motifs.

A short sequence in the C-terminal cytoplasmic portion of MARCH1 is important for its activity

As the tyrosine motifs are dispensable for the function of human MARCH1 in our experimental system, we asked whether the N-terminal cytoplasmic tail bearing the RING domain would be sufficient to downregulate MHC II molecules. To test this possibility, we truncated the entire cytoplasmic C-terminal portion (ΔCter; Fig. 1A,B). Despite this large deletion, M1ΔCter still colocalized with CD63 and associated with MHC II molecules (Fig. 6A,B). However, M1ΔCter was inactive and unable to downregulate MHC II molecules in CIITA^{+} HEK 293E cells (Fig. 6C). To better define the minimal region needed to complement the RING domain and knowing that the Δ42 construct was fully active (Fig. 1D), we generated two truncated molecules that shortened the C-terminal of another 6 (Δ48) or 9 (Δ51) residues (Fig. 1A,B). As expected, these mutants also co-localized with CD63 (Fig. 6A). Interestingly, as compared to M1Δ48, the Δ51 mutant showed a dramatic reduction in its ability to downregulate MHC II surface expression, suggesting that this region contains key functional elements (Fig. 6C). These results confirm those of Jabbour et al. who showed that deletion of the last 50 C-terminal amino acids abrogated the activity of mMARCH1 (Jabbour et al., 2009).

Valine 221 is important for the function of MARCH1

To better characterize the region comprised between the Δ51 and Δ48 deletion mutants, we made alanine substitutions at positions Q222, N223 and C224. Interestingly, none of these mutants was impaired in its ability to downregulate cell surface MHC II molecules in transfected HEK 293E CIITA cells (Fig. 7A). The weaker expression of the N223A mutant was not observed in independent transfections (data not shown). These results suggest that the important residues are most likely located in the vicinity of the C-terminus in the Δ51 mutant. Alternatively, the secondary structure of this short 222–224 region may be more important than the nature of the specific amino acids. To investigate these possibilities, we tested a triple mutant (M1VQN-AAA) and one in which only the V221 position was modified (M1V221A). Interestingly, mutation of the valine 221 was sufficient to reduce the activity of the enzyme (Fig. 7B). The triple VQN-AAA mutation and the Δ51 deletion appeared even more deleterious than the single V221A mutation, suggesting that the whole $_{221}$VQNC$_{224}$ stretch is important.

Mutation of valine 221 affects conformation of the cytoplasmic tails

A blast of the human genome revealed the presence of VQNC motifs in other proteins, including the RING-type E3 ubiquitin ligases arkadia and parkin (Miyazono and Koinuma, 2011; Rankin et al., 2011). Parkin is a 465 amino acid protein with an ubiquitin-like (UBL) domain at its N-terminus and two RING finger domains (Rankin et al., 2011). Of note, substitution of the valine for a glutamic acid in the VQNC motif of parkin is associated with the development of Parkinson disease (Hoenicka et al., 2002). Flow cytometry experiments in transfected HEK 293E CIITA cells showed that replacement of V221 in MARCH1 by a glutamate (M1V221E) had the same, even greater, effect as the alanine substitution on the activity of MARCH1 (Fig. 8A). The role of the VQNC stretch in parkin has not been investigated at the molecular level but it appears that the pathogenic V56E mutation might affect the half-life of the protein (Henn et al., 2005). To investigate the possibility that the substitution of the V221 resulted in a decreased stability of the protein that would

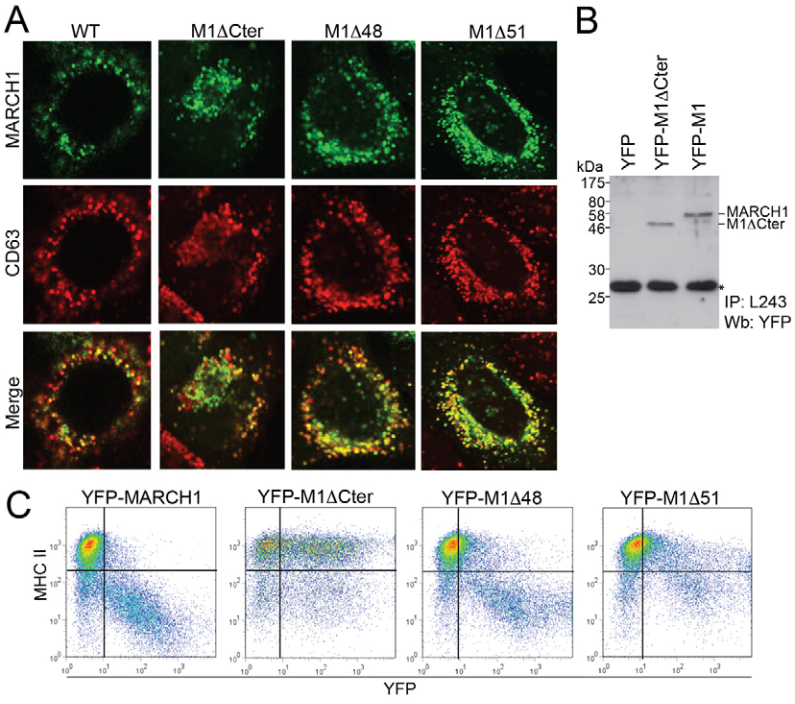

Fig. 6. The C-terminal cytoplasmic portion of MARCH1 contains a short sequence that is essential for its function in relation to MHC II. (**A**) Confocal microscopy analysis of HeLa cells transfected with YFP-MARCH1, YFP-M1Δ48, YFP-M1Δ51 or YFP-M1ΔCter and stained for CD63. (**B**) Western blot analysis of YFP-tagged proteins co-immunoprecipitated with L243 from HEK 293E CIITA cells transfected with YFP, YFP-M1ΔCter or YFP-M1. (**C**) HEK 293E cells were transfected with YFP-MARCH1, YFP-M1ΔCter, YFP-M1Δ48 or YFP-M1Δ51 and analyzed by flow cytometry. The dot plots show the surface expression of DR relative to YFP fluorescence. Data are representative of at least four different experiments.

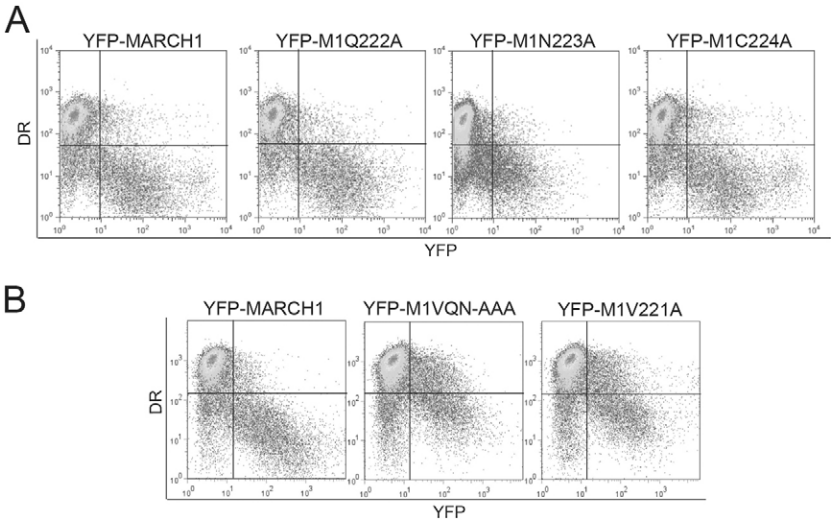

Fig. 7. Valine 221 is important for the function of MARCH1. (**A**) HEK 293E CIITA cells were transfected with YFP-MARCH1, YFP-M1Q222A, YFP-M1N223A or YFP-M1C224A and analyzed by flow cytometry. The dot plots show the surface expression of DR relative to YFP expression. (**B**) HEK 293E CIITA cells were transfected with YFP-MARCH1, YFP-M1VQN-AAA or YFP-M1V221A and analyzed by flow cytometry. The dot plots show the surface expression of DR relative to YFP expression. Data are representative of two (A) and three (B) different experiments.

lead to its premature degradation, we assessed the degradation kinetic of MARCH1 and the two V221 mutants. To do so, HEK 293T cells were transfected with YFP-MARCH1, YFP-M1V221A or YFP-M1V221E, treated for different periods of time with cycloheximide to prevent protein synthesis and the MFVs were determined by flow cytometry (Fig. 8B). The results showed no significant difference in the stability of MARCH1 and the two V221 mutants.

In MARCH1, we noted that the V221 residue is located 19 amino acids away from the end of the second TM region (Fig. 1A). Although the ternary structure of the cytoplasmic domains is unknown, it is possible that the V221 interacts with the RING domain, which starts 21 residues from the plasma membrane on the juxtaposed N-terminal cytoplasmic region. To investigate whether the V221A change could modify the relative orientation of the two cytoplasmic tails, we performed a bioluminescence resonance energy transfer (BRET) experiment between two different tags attached at each extremity of the MARCH1 molecule. YFP was attached to the N-terminus of MARCH1 while Rluc was linked to the C-terminus of the same molecule. The efficiency of energy transfer between the luciferase substrate and YFP was monitored in HEK 293T cells transfected with the tagged MARCH1 or M1V221A mutant. We found that the BRET ratio was significantly reduced for the V221A (Fig. 8C) and V221E mutants (data not shown). These results demonstrate that the spatial orientation of the two cytoplasmic tails is modified and that the two tags are further apart in the MARCH1 mutants.

Discussion

MARCH1 is found at extremely low levels in primary cells, suggesting that its deregulated expression or activity can be detrimental to the cell. To further characterize the mode of action of MARCH1, we first looked for the site of interaction with MHC II. Our FRET experiments demonstrated the colocalization of MARCH1 and MHC II in cytoplasmic vesicles (Fig. 2A). Although Eyster et al. were able to detect some MARCH1 at the plasma membrane, it is well established that MARCH1 is mainly localized in the endocytic pathway (Bartee et al., 2004; Eyster et al., 2011). Thus, our results are in line with a model in

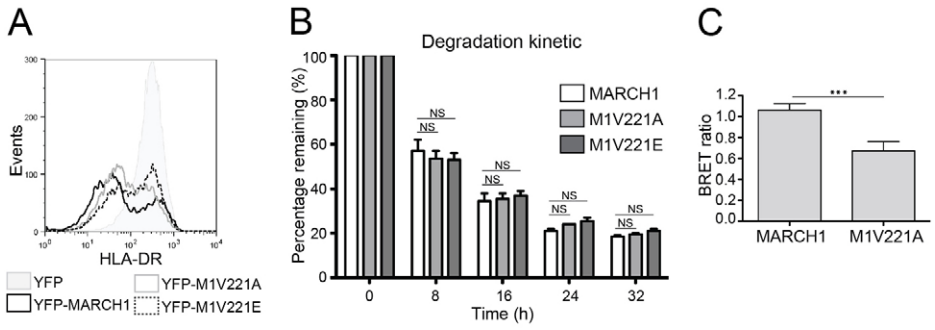

Fig. 8. The V221 residue of MARCH1 influences the spatial orientation of the cytoplasmic tails. (**A**) HEK 293E CIITA cells were transfected with YFP-MARCH1, YFP-M1V221A or YFP-M1V221E and analyzed by flow cytometry for cell surface MHC II expression. (**B**) HEK 293T cells were transfected with YFP-MARCH1, YFP-M1V221A or YFP-M1V221E. After 48 hours, the cells were incubated with cycloheximide and analyzed at different time points by flow cytometry for YFP expression. The MFVs were averaged from two independent transfections and time 0 was considered as 100%. (**C**) HEK 293T cells were transfected with YFP-MARCH1-Rluc or YFP-M1V221A-Rluc. The fluorescence and the luminescence emitted by the cells were measured before and after the addition of coelenterazine H. The BRET ratio was calculated by dividing the fluorescence (the value with substrate subtracted from the value without substrate) by the luminescence values. The results are represented as a bar chart and are from two independent experiments. Student's *t*-test was performed; ***$P \leq 0.1$; NS, no significant difference.

which MARCH1 would not affect the endocytosis of the target molecules but would rather regulate trafficking inside the endocytic pathway (Eyster et al., 2011).

Two studies demonstrated the presence of functional tyrosine-based motifs in the C-terminal region of murine MARCH1 and human MARCH8 (Goto et al., 2008; Jabbour et al., 2009). These signals do not appear to be so critical for human MARCH1, at least when testing for the modulation of MHC II expression (Fig. 4B,C). This result is surprising as the mouse and human MARCH1 molecules show only eight amino acids differences in their C-terminal cytoplasmic tails. Interestingly, we have shown that MARCH1 was incorporated into exosomes, a process that was less efficient when the tyrosine motifs were mutated (Fig. 5B). Tyrosine-based endosomal sorting motifs are known to trigger the incorporation of many cargo proteins into exosomes, including the transferrin receptor (Géminard et al., 2004). We cannot rule out the possibility that the tyrosine motifs exert an indirect effect by regulating the capacity of MARCH1 to get ubiquitylated (Bourgeois-Daigneault and Thibodeau, 2012). This post-translational modification is known to modulate the incorporation of many proteins into exosomes (Buschow et al., 2005). There is an increasing number of studies reporting the inter-cellular transport of material via exosomes (Simons and Raposo, 2009; Mathivanan et al., 2010; Escrevente et al., 2011). If MARCH1 from IL-10-responsive DCs can be transferred in exosomes to regulate the cell surface display of specific targets in distant APCs remains to be determined (Quah and O'Neill, 2005).

The search for functional domains allowed the identification of a critical amino acid sequence close to the C-terminal tyrosine motifs. The VQNC stretch, including the critical V221 residue, appears to be in close proximity of the RING domain located on the other cytoplasmic tail. Structural alterations in this region might affect the binding site for important proteins in the ubiquitylation complex, such as an E2. However, the V221 point mutants are still partially active and preliminary mass spectrometry analyses following pull-down experiments did not reveal qualitative differences in the co-immunoprecipitated material (data not shown). We previously demonstrated that MARCH1 form dimers that were required for its autoregulation (Bourgeois-Daigneault and Thibodeau, 2012). However, the implication of MARCH1 dimers in its activity is not known. One could argue that the 'VQNC' motif might be involved in dimer formation. However, our results showed that dimerization was not impaired in the absence of the C-terminal cytoplasmic portion (Bourgeois-Daigneault and Thibodeau, 2012). Thus, it is unlikely that the VQNC sequence is implicated in the oligomerization of MARCH1. Our BRET analysis rather suggested that the V221 is somewhat buried into the 3D structure of the enzyme and that its mutation affects the overall conformation of the cytoplasmic tails. Although the sequence VQNC can be found in many proteins, it is interesting to note that it is present in the E3 ligase parkin. This cytoplasmic protein has two RING-finger motifs separated by an IBR (in-between RING fingers) region (Rankin et al., 2011). Its N-terminal region contains a UBL domain, which includes the $_{56}$VQNC$_{59}$ motif. Most importantly, the V56 residue is changed for a glutamate in a family with recessive inheritance of Parkinson disease (Hoenicka et al., 2002; Kahle and Haass, 2004). The V56 residue lines the short α2 helical region composed of four residues, including the QNC stretch (Sakata et al., 2003). The V56 side chain points toward the interior of the domain and its substitution probably affects the orientation of the exposed α2 helix. In line with our BRET and cycloheximide-chase experiments on MARCH1 (Fig. 8B,C), a study by the group of Ishida showed that mutation of the parkin V56 residue influenced the flexibility, but not the stability of the protein (Tomoo et al., 2008). There is no structural homology between the C-terminal cytoplasmic tail of MARCH1 and UBLs according to the Structure Prediction Meta Server (Bujnicki et al., 2001). Still, the possibility remains that some short structural features, such as the VQNC sequence, act like specific sub-regions of UBL domains. Indeed, the N-terminal UBL domain of parkin has been ascribed many different functions. For example, it binds the S5a proteasomal subunit to facilitate the degradation of parkin's substrates (Sakata et al., 2003). Also, the UBL domain interacts with Eps15, a multifunctional adaptor which binds ubiquitin and regulates endocytosis as well as intracellular trafficking of various cargo proteins (Fallon et al., 2006; van Bergen En Henegouwen, 2009). Future experiments will address the capacity of MARCH1 to interact with such ubiquitin-interacting motif (UIM) proteins. Another possible role for the MARCH1 VQNC motif could be in the autoregulation of the enzymatic activity. The UBL domain of parkin was proposed to fold close to the RING domain and to inhibit autoubiquitylation (Chaugule et al., 2011). Our BRET analysis showing the altered conformation of MARCH1 is in line with an interaction between the two cytoplasmic tails.

MARCH1 is a relatively small protein but as a multipass integral membrane protein, its tertiary structure promises to be difficult to resolve. Our results and those of Jabbour et al. showed the presence of multiple functional domains, highlighting the complexity of using ubiquitin as a regulatory mechanism of protein expression and trafficking (Jabbour et al., 2009). Moreover, the list of MARCH1 targets is likely to expand in the near future and new functions for MARCH1 may emerge (Bartee et al., 2010). Further studies are warranted to fully characterize the structure-function aspects of ubiquitylation by MARCH proteins.

Materials and Methods

Antibodies

Mouse IgG_1 XD5 (recognizes the DRβ chain), mouse IgG_{2a} L243 (recognizes the HLA-DRα chain in the context of the heterodimer) and mouse IgG2b ISCR3 (recognizes the HLA-DR heterodimer) have been described previously (Khalil et al., 2005). For the immunofluorescence microscopy experiments, we used the anti-Lamp-1 (H5C6; mouse IgG_1) and anti-CD63 from the Developmental Studies Hybridoma Bank (NICHD, University of Iowa, IA). The anti-calnexine and Alexa-Fluor-594-coupled goat anti-mouse antibodies were purchased from Invitrogen (Laval, Canada).

Reagents

Polyethyleimine (2.5 kDa linear) was obtained from Polysciences Inc. (Warrington, PA, USA). Cycloheximide (Sigma-Aldrich, Oakville, ON, Canada) was used at a final concentration of 100 μg/ml. Lipofectamine, Plus reagent and Hoechst 33342 were purchased from Invitrogen (Laval, Canada). A complete protease inhibitors cocktail (Roche, Laval, QC, Canada), endoglycosidase H (New England Biolabs, Ontario, Canada) and coelenterazine H (Nanolight Technology, Pinetop, AZ, USA) were used according to the manufacturer's recommendations.

Plasmids and mutagenesis

$EGFP_2$-MARCH, EYFP-MARCH1 and EYFP-MARCH8 plasmids were obtained by fusing $EGFP_2$ or EYFP to the N-terminus of MARCH1 by the PCR overlapping method using the pcDNA3.1_ $EGFP_2$_MCS or the pcDNA3.1_EYFP_MCS plasmids (Bourgeois-Daigneault and Thibodeau, 2012). DRβ-EYFP and DRβ-$EGFP_2$ were obtained by fusing the EYFP or $EGFP_2$ to the C-terminus of DRβ by the same method using the pcDNA3.1_MCS_EYFP or the pcDNA3.1_MCS_ $EGFP_2$ plasmids. The DRβ-M1 and DRβ-M1YY were constructed by fusing DRβ (methionine 1 to arginine 251) to human MARCH1 or M1YY, respectively

(glutamine 201 to valine 272). The chimeric molecule was generated by PCR overlap and cloned in the *Bsi*W1 and *Not*I restriction sites of pcDNA3.1_MCS. The M1Y205F, M1Y215F, M1YY (Y205F and Y215F), M1V221A, M1V221E, M1Q222A, M1N223A, M1C224A and M1VQN-AAA were obtained by mutating the corresponding residues by PCR overlap. The $M1_{KKxx}$, M1Δ42, M1Δ48, M1Δ51 and M1ΔCter were obtained by the addition of a stop codon after the triplets coding for glutamic acid 232, lysine 230, cystein 224, valine 221 or cysteine 202, respectively. The M8ΔRING was obtained by deleting the first 126 amino acids and by adding a methionine before the triplet coding for lysine 127 of wild-type MARCH8. The EYFP-MARCH1-Rluc and EYFP-M1V221A-Rluc were obtained by fusing EYFP-MARCH1 or EYFP-M1V221A to the N-terminus of Rluc by PCR overlap using the pcDNA3.1_MCS_Rluc.

Cell culture and transfections

HEK293T, HEK 293E CIITA, HeLa and HeLa DR1 cells were cultured in DMEM supplemented with 5% FBS (Wisent, Saint-Jean Baptiste, QC, Canada). HEK 293T cells were transfected using 3 µg of polyethyleimine per microgram of DNA, as described previously (Bourgeois-Daigneault and Thibodeau, 2012). HeLa cells were transfected using Lipofectamine Plus reagent, according to the manufacturer's protocol (Invitrogen, Laval, Canada).

Immunofluorescence microscopy

HeLa cells were plated on coverslips 24 hours prior to transfection. Cells were transfected and incubated for 48 hours. Cells were then fixed, permeabilized and stained on coverslips. Samples were analyzed on a LSM 510 Meta Zeiss confocal microscope.

For FRET experiments, 5×10^5 cells were plated and transfected on 35 mm glass-bottomed dishes (MatTek, Ashland, MA, USA) 48 hours prior to the experiment. Images of living cells were taken using a LSM Meta Zeiss confocal microscope. For $EGFP_2$, the cells were excited at a 405 nm wavelength and the signal was detected by using a 470–500 nm band-pass filter. For YFP, cells were scanned at 488 nm with a 560 nm long-pass filter and the FRET signal was detected at 530–560 nm upon excitation at 405 nm.

Exosome purification and analysis

HEK 293E cells in ten 10 cm Petri dishes per condition were transfected and the medium was changed for exosome-free medium after 24 hours. Cells were cultured for 24 hours and the medium was collected. Exosomes were purified by ultracentrifugation and coupled to latex beads for flow cytometry analysis, as described previously (Gauvreau et al., 2009).

Flow cytometry

For cell surface stainings, the cells were harvested and incubated with primary antibodies in PBS for 30 minutes on ice. The cells were washed three times with ice-cold PBS prior to incubation with a secondary antibody in PBS for 30 minutes on ice. The cells were washed three more times with ice-cold PBS and analyzed on a FACS-Calibur instrument (Becton Dickinson, CA).

For total protein stainings, all the steps were performed at room temperature as described previously (Brunet et al., 2000).

For endocytosis experiments, the cells were transfected for 48 hours and incubated with the MHC II-specific L243 primary antibody. The cells were washed three times with ice-cold PBS and incubated at 37℃. At each time point, a cell aliquot was fixed with a solution of 1% PFA in ice-cold PBS. When all samples were ready, the cells were washed with ice-cold PBS and stained with the secondary antibody for flow cytometry, as described above.

Bioluminescence resonance energy transfer

HEK 293T cells were transfected with YFP-MARCH1-Rluc or YFP-M1V221A-Rluc 48 hours prior to the experiment. Cells were harvested, washed, and 10^5 cells per condition were plated in duplicate in a 96-well plate. The background fluorescence was determined before the addition of coelenterazine at a concentration of 5 µM. The luminescence and fluorescence intensities were determined using a Mithras LB940 spectrofluorometer (Berthold Technologies, Bad Wildbad, Germany) and multiplate reader with the settings described previously (Bourgeois-Daigneault and Thibodeau, 2012). The BRET ratio was calculated by dividing the acceptor-emitted fluorescence by the donor-emitted luminescence. BRET ratios were normalized by subtracting the background signal from cells transfected without YFP.

Western blot analysis

Cells were lysed in 1% Triton X-100 lysis buffer complemented with complete protease inhibitor cocktail. Post-nuclear supernatants were analyzed by SDS-PAGE in reducing conditions. Proteins were transferred to Hybond ECL membrane (GE Healthcare, Mississauga, ON, Canada) and analyzed with the rabbit anti-CLIP antibody. Goat anti-rabbit coupled to peroxidase antibody (Bio/Can Scientific) was used and detected using a chemiluminescence blotting substrate (POD) from Roche (Laval, Quebec, Canada).

Acknowledgements

We thank Jonathan Boulais for help with bioinformatic analyses and Edward Fon and Jean-François Trempe for helpful discussions. We also thank Peter Cresswell for antibodies and the Developmental Studies Hybridoma Bank for the CD63 (under the auspices of the NICHD, National Institutes of Health, and is maintained by the University of Iowa, Department of Biological Sciences, Iowa City, IA 52242).

Author contributions

M.-C.B.-D. performed all experiments, analyzed the data and wrote the paper. J.T. wrote the paper.

Funding

This work was supported by the Canadian Institutes of Health Research [grant number 36355 to J.T.]; and scholarships from the Cole Foundation and the University of Montreal to M.-C.B.-D.

References

Adhikari, A. and Chen, Z. J. (2009). Diversity of polyubiquitin chains. *Dev. Cell* **16**, 485-486.

Bartee, E., Mansouri, M., Hovey Nerenberg, B. T., Gouveia, K. and Früh, K. (2004). Downregulation of major histocompatibility complex class I by human ubiquitin ligases related to viral immune evasion proteins. *J. Virol.* **78**, 1109-1120.

Bartee, E., Eyster, C. A., Viswanathan, K., Mansouri, M., Donaldson, J. G. and Früh, K. (2010). Membrane-Associated RING-CH proteins associate with Bap31 and target CD81 and CD44 to lysosomes. *PLoS ONE* **5**, e15132.

Berger, A. C. and Roche, P. A. (2009). MHC class II transport at a glance. *J. Cell Sci.* **122**, 1-4.

Boname, J. M., de Lima, B. D., Lehner, P. J. and Stevenson, P. G. (2004). Viral degradation of the MHC class I peptide loading complex. *Immunity* **20**, 305-317.

Bourgeois-Daigneault, M.-C. and Thibodeau, J. (2012). Autoregulation of MARCH1 expression by dimerization and autoubiquitination. *J. Immunol.* **188**, 4959-4970.

Brachet, V., Péhau-Arnaudet, G., Desaymard, C., Raposo, G. and Amigorena, S. (1999). Early endosomes are required for major histocompatiblity complex class II transport to peptide-loading compartments. *Mol. Biol. Cell* **10**, 2891-2904.

Brunet, A., Samaan, A., Deshaies, F., Kindt, T. J. and Thibodeau, J. (2000). Functional characterization of a lysosomal sorting motif in the cytoplasmic tail of HLA-DObeta. *J. Biol. Chem.* **275**, 37062-37071.

Bujnicki, J. M., Elofsson, A., Fischer, D. and Rychlewski, L. (2001). Structure prediction meta server. *Bioinformatics* **17**, 750-751.

Buschow, S. I., Liefhebber, J. M. P., Wubbolts, R. and Stoorvogel, W. (2005). Exosomes contain ubiquitinated proteins. *Blood Cells Mol. Dis.* **35**, 398-403.

Cadwell, K. and Coscoy, L. (2008). The specificities of Kaposi's sarcoma-associated herpesvirus-encoded E3 ubiquitin ligases are determined by the positions of lysine or cysteine residues within the intracytoplasmic domains of their targets. *J. Virol.* **82**, 4184-4189.

Chaugule, V. K., Burchell, L., Barber, K. R., Sidhu, A., Leslie, S. J., Shaw, G. S. and Walden, H. (2011). Autoregulation of Parkin activity through its ubiquitin-like domain. *EMBO J.* **30**, 2853-2867.

Corcoran, K., Jabbour, M., Bhagwandin, C., Deymier, M. J., Theisen, D. L. and Lybarger, L. (2011). Ubiquitin-mediated regulation of CD86 protein expression by the ubiquitin ligase membrane-associated RING-CH-1 (MARCH1). *J. Biol. Chem.* **286**, 37168-37180.

Cresswell, P. (1996). Invariant chain structure and MHC class II function. *Cell* **84**, 505-507.

De Gassart, A., Camosseto, V., Thibodeau, J., Ceppi, M., Catalan, N., Pierre, P. and Gatti, E. (2008). MHC class II stabilization at the surface of human dendritic cells is the result of maturation-dependent MARCH I down-regulation. *Proc. Natl. Acad. Sci. USA* **105**, 3491-3496.

Denzin, L. K. and Cresswell, P. (1995). HLA-DM induces CLIP dissociation from MHC class II α β dimers and facilitates peptide loading. *Cell* **82**, 155-165.

Deshaies, R. J. and Joazeiro, C. A. P. (2009). RING domain E3 ubiquitin ligases. *Annu. Rev. Biochem.* **78**, 399-434.

Dugast, M., Toussaint, H., Dousset, C. and Benaroch, P. (2005). AP2 clathrin adaptor complex, but not AP1, controls the access of the major histocompatibility complex (MHC) class II to endosomes. *J. Biol. Chem.* **280**, 19656-19664.

Escrevente, C., Keller, S., Altevogt, P. and Costa, J. (2011). Interaction and uptake of exosomes by ovarian cancer cells. *BMC Cancer* **11**, 108.

Eyster, C. A., Cole, N. B., Petersen, S., Viswanathan, K., Früh, K. and Donaldson, J. G. (2011). MARCH ubiquitin ligases alter the itinerary of clathrin-independent cargo from recycling to degradation. *Mol. Biol. Cell* **22**, 3218-3230.

Fallon, L., Bélanger, C. M. L., Corera, A. T., Kontogiannea, M., Regan-Klapisz, E., Moreau, F., Voortman, J., Haber, M., Rouleau, G., Thorarinsdottir, T. et al. (2006). A regulated interaction with the UIM protein Eps15 implicates parkin in EGF receptor trafficking and PI(3)K-Akt signalling. *Nat. Cell Biol.* **8**, 834-842.

Galbas, T., Steimle, V., Lapointe, R., Ishido, S. and Thibodeau, J. (2012). MARCH1 down-regulation in IL-10-activated B cells increases MHC class II expression. *Cytokine* **59**, 27-30.

Gauvreau, M.-E., Côté, M.-H., Bourgeois-Daigneault, M.-C., Rivard, L. D., Xiu, F., Brunet, A., Shaw, A., Steimle, V. and Thibodeau, J. (2009). Sorting of MHC class II molecules into exosomes through a ubiquitin-independent pathway. *Traffic* **10**, 1518-1527.

Géminard, C., De Gassart, A., Blanc, L. and Vidal, M. (2004). Degradation of AP2 during reticulocyte maturation enhances binding of hsc70 and Alix to a common site on TFR for sorting into exosomes. *Traffic* **5**, 181-193.

Goto, E., Mito-Yoshida, M., Uematsu, M., Aoki, M., Matsuki, Y., Ohmura-Hoshino, M., Hotta, H., Miyagishi, M. and Ishido, S. (2008). An excellent monitoring system for surface ubiquitination-induced internalization in mammals. *PLoS ONE* **3**, e1490.

Henn, I. H., Gostner, J. M., Lackner, P., Tatzelt, J. and Winklhofer, K. F. (2005). Pathogenic mutations inactivate parkin by distinct mechanisms. *J. Neurochem.* **92**, 114-122.

Hoenicka, J., Vidal, L., Morales, B., Ampuero, I., Jiménez-Jiménez, F. J., Berciano, J., del Ser, T., Jiménez, A., Ruíz, P. G. and de Yébenes, J. G. (2002). Molecular findings in familial Parkinson disease in Spain. *Arch. Neurol.* **59**, 966-970.

Hsing, L. C. and Rudensky, A. Y. (2005). The lysosomal cysteine proteases in MHC class II antigen presentation. *Immunol. Rev.* **207**, 229-241.

Ishido, S., Goto, E., Matsuki, Y. and Ohmura-Hoshino, M. (2009). E3 ubiquitin ligases for MHC molecules. *Curr. Opin. Immunol.* **21**, 78-83.

Jabbour, M., Campbell, E. M., Fares, H. and Lybarger, L. (2009). Discrete domains of MARCH1 mediate its localization, functional interactions, and posttranscriptional control of expression. *J. Immunol.* **183**, 6500-6512.

Jahnke, M., Trowsdale, J., and Kelly, A. P. (2012). Ubiquitination of human leukocyte antigen (HLA)-DM by different membrane-associated RING-CH (MARCH) protein family e3 ligases targets different endocytic pathways. *J. Biol. Chem.* **287**, 7256-7264.

Kahle, P. J. and Haass, C. (2004). How does parkin ligate ubiquitin to Parkinson's disease? *EMBO Rep.* **5**, 681-685.

Khalil, H., Brunet, A. and Thibodeau, J. (2005). A three-amino-acid-long HLA-DRbeta cytoplasmic tail is sufficient to overcome ER retention of invariant-chain p35. *J. Cell Sci.* **118**, 4679-4687.

Kreft, S. G., Wang, L. and Hochstrasser, M. (2006). Membrane topology of the yeast endoplasmic reticulum-localized ubiquitin ligase Doa10 and comparison with its human ortholog TEB4 (MARCH-VI). *J. Biol. Chem.* **281**, 4646-4653.

Landsverk, O. J. B., Bakke, O. and Gregers, T. F. (2009). MHC II and the endocytic pathway: regulation by invariant chain. *Scand. J. Immunol.* **70**, 184-193.

Lehner, P. J., Hoer, S., Dodd, R. and Duncan, L. M. (2005). Downregulation of cell surface receptors by the K3 family of viral and cellular ubiquitin E3 ligases. *Immunol. Rev.* **207**, 112-125.

Manoury, B., Mazzeo, D., Li, D. N., Billson, J., Loak, K., Benaroch, P. and Watts, C. (2003). Asparagine endopeptidase can initiate the removal of the MHC class II invariant chain chaperone. *Immunity* **18**, 489-498.

Mathivanan, S., Ji, H. and Simpson, R. J. (2010). Exosomes: extracellular organelles important in intercellular communication. *J. Proteomics* **73**, 1907-1920.

Matsuki, Y., Ohmura-Hoshino, M., Goto, E., Aoki, M., Mito-Yoshida, M., Uematsu, M., Hasegawa, T., Koseki, H., Ohara, O., Nakayama, M. et al. (2007). Novel regulation of MHC class II function in B cells. *EMBO J.* **26**, 846-854.

McCormick, P. J., Martina, J. A. and Bonifacino, J. S. (2005). Involvement of clathrin and AP-2 in the trafficking of MHC class II molecules to antigen-processing compartments. *Proc. Natl. Acad. Sci. USA* **102**, 7910-7915.

Miyazono, K. and Koinuma, D. (2011). Arkadia—beyond the TGF-β pathway. *J. Biochem.* **149**, 1-3.

Nathan, J. A. and Lehner, P. J. (2009). The trafficking and regulation of membrane receptors by the RING-CH ubiquitin E3 ligases. *Exp. Cell Res.* **315**, 1593-1600.

Nilsson, T., Jackson, M. and Peterson, P. A. (1989). Short cytoplasmic sequences serve as retention signals for transmembrane proteins in the endoplasmic reticulum. *Cell* **58**, 707-718.

Ohmura-Hoshino, M., Goto, E., Matsuki, Y., Aoki, M., Mito, M., Uematsu, M., Hotta, H. and Ishido, S. (2006). A novel family of membrane-bound E3 ubiquitin ligases. *J. Biochem.* **140**, 147-154.

Quah, B. J. C. and O'Neill, H. C. (2005). The immunogenicity of dendritic cell-derived exosomes. *Blood Cells Mol. Dis.* **35**, 94-110.

Rankin, C. A., Roy, A., Zhang, Y. and Richter, M. (2011). Parkin, a top level manager in the cell's Sanitation Department. *Open Biochem. J.* **5**, 9-26.

Sakata, E., Yamaguchi, Y., Kurimoto, E., Kikuchi, J., Yokoyama, S., Yamada, S., Kawahara, H., Yokosawa, H., Hattori, N., Mizuno, Y. et al. (2003). Parkin binds the Rpn10 subunit of 26S proteasomes through its ubiquitin-like domain. *EMBO Rep.* **4**, 301-306.

Salamero, J., Le Borgne, R., Saudrais, C., Goud, B. and Hoflack, B. (1996). Expression of major histocompatibility complex class II molecules in HeLa cells promotes the recruitment of AP-1 Golgi-specific assembly proteins on Golgi membranes. *J. Biol. Chem.* **271**, 30318-30321.

Shin, J.-S., Ebersold, M., Pypaert, M., Delamarre, L., Hartley, A. and Mellman, I. (2006). Surface expression of MHC class II in dendritic cells is controlled by regulated ubiquitination. *Nature* **444**, 115-118.

Simons, M. and Raposo, G. (2009). Exosomes—vesicular carriers for intercellular communication. *Curr. Opin. Cell Biol.* **21**, 575-581.

Szöllosi, J., Damjanovich, S. and Mátyus, L. (1998). Application of fluorescence resonance energy transfer in the clinical laboratory: routine and research. *Cytometry* **34**, 159-179.

ten Broeke, T., van Niel, G., Wauben, M. H. M., Wubbolts, R. and Stoorvogel, W. (2011). Endosomally stored MHC class II does not contribute to antigen presentation by dendritic cells at inflammatory conditions. *Traffic* **12**, 1025-1036.

Théry, C., Zitvogel, L. and Amigorena, S. (2002). Exosomes: composition, biogenesis and function. *Nat. Rev. Immunol.* **2**, 569-579.

Thibodeau, J., Bourgeois-Daigneault, M.-C., Huppé, G., Tremblay, J., Aumont, A., Houde, M., Bartee, E., Brunet, A., Gauvreau, M. E., de Gassart, A. et al. (2008). Interleukin-10-induced MARCH1 mediates intracellular sequestration of MHC class II in monocytes. *Eur. J. Immunol.* **38**, 1225-1230.

Tomoo, K., Mukai, Y., In, Y., Miyagawa, H., Kitamura, K., Yamano, A., Shindo, H. and Ishida, T. (2008). Crystal structure and molecular dynamics simulation of ubiquitin-like domain of murine parkin. *Biochim. Biophys. Acta* **1784**, 1059-1067.

Tze, L. E., Horikawa, K., Domaschenz, H., Howard, D. R., Roots, C. M., Rigby, R. J., Way, D. A., Ohmura-Hoshino, M., Ishido, S., Andoniou, C. E. et al. (2011). CD83 increases MHC II and CD86 on dendritic cells by opposing IL-10-driven MARCH1-mediated ubiquitination and degradation. *J. Exp. Med.* **208**, 149-165.

van Bergen En Henegouwen, P. (2009). Eps15: a multifunctional adaptor protein regulating intracellular trafficking. *Cell Commun. Signal.* **7**, 24.

van Niel, G., Wubbolts, R., Ten Broeke, T., Buschow, S. I., Ossendorp, F. A., Melief, C. J., Raposo, G., van Balkom, B. W. and Stoorvogel, W. (2006). Dendritic cells regulate exposure of MHC class II at their plasma membrane by oligoubiquitination. *Immunity* **25**, 885-894.

Walseng, E., Bakke, O. and Roche, P. A. (2008). Major histocompatibility complex class II-peptide complexes internalize using a clathrin- and dynamin-independent endocytosis pathway. *J. Biol. Chem.* **283**, 14717-14727.

Walseng, E., Furuta, K., Bosch, B., Weih, K. A., Matsuki, Y., Bakke, O., Ishido, S. and Roche, P. A. (2010). Ubiquitination regulates MHC class II-peptide complex retention and degradation in dendritic cells. *Proc. Natl. Acad. Sci. USA* **107**, 20465-20470.

Wang, X., Herr, R. A. and Hansen, T. (2008). Viral and cellular MARCH ubiquitin ligases and cancer. *Semin. Cancer Biol.* **18**, 441-450.

Ye, Y. and Rape, M. (2009). Building ubiquitin chains: E2 enzymes at work. *Nat. Rev. Mol. Cell Biol.* **10**, 755-764.